
جامعة الملك عبدالله
للعلوم والتقنية
King Abdullah University of
Science and Technology

Enhanced carrier density in Nb-doped SrTiO3 thermoelectrics

Item Type	Article
Authors	Ozdogan, K.; Upadhyay Kahaly, M.; Sarath Kumar, S. R.; Alshareef, Husam N.; Schwingenschlögl, Udo
Citation	Enhanced carrier density in Nb-doped SrTiO3 thermoelectrics 2012, 111 (5):054313 Journal of Applied Physics
Eprint version	Publisher's Version/PDF
DOI	10.1063/1.3692057
Publisher	AIP Publishing
Journal	Journal of Applied Physics
Rights	Archived with thanks to Journal of Applied Physics
Download date	25/02/2022 11:50:00
Link to Item	http://hdl.handle.net/10754/552834

AIP Journal of Applied Physics

Enhanced carrier density in Nb-doped SrTiO3 thermoelectrics

K. Ozdogan, M. Upadhyay Kahaly, S. R. Sarath Kumar, H. N. Alshareef, and U. Schwingenschlögl

Citation: Journal of Applied Physics **111**, 054313 (2012); doi: 10.1063/1.3692057
View online: http://dx.doi.org/10.1063/1.3692057
View Table of Contents: http://scitation.aip.org/content/aip/journal/jap/111/5?ver=pdfcov
Published by the AIP Publishing

Articles you may be interested in

Density functional theory and experimental study of the electronic structure and transport properties of La, V, Nb, and Ta doped SrTiO3
J. Appl. Phys. **113**, 013701 (2013); 10.1063/1.4770360

Anomalous enhancement of the thermoelectric figure of merit by V co-doping of Nb-SrTiO3
Appl. Phys. Lett. **100**, 193110 (2012); 10.1063/1.4714541

Electronic transport behavior of off-stoichiometric La and Nb doped SrxTiyO3−δ epitaxial thin films and donor doped single-crystalline SrTiO3
Appl. Phys. Lett. **99**, 232111 (2011); 10.1063/1.3664397

Preparation and thermoelectric properties of heavily Nb-doped SrO (SrTiO 3) 1 epitaxial films
J. Appl. Phys. **102**, 033702 (2007); 10.1063/1.2764221

High-temperature carrier transport and thermoelectric properties of heavily La- or Nb-doped Sr Ti O 3 single crystals
J. Appl. Phys. **97**, 034106 (2005); 10.1063/1.1847723

MIT LINCOLN LABORATORY CAREERS

Discover the satisfaction of innovation and service to the nation

- Space Control
- Air & Missile Defense
- Communications Systems & Cyber Security
- Intelligence, Surveillance and Reconnaissance Systems
- Advanced Electronics
- Tactical Systems
- Homeland Protection
- Air Traffic Control

LINCOLN LABORATORY
MASSACHUSETTS INSTITUTE OF TECHNOLOGY



[This article is copyrighted as indicated in the article. Reuse of AIP content is subject to the terms at: http://scitation.aip.org/termsconditions. Downloaded to] IP: 109.171.137.210 On: Mon, 11 May 2015 07:14:12

Enhanced carrier density in Nb-doped $SrTiO_3$ thermoelectrics

K. Ozdogan,[1,2] M. Upadhyay Kahaly,[1] S. R. Sarath Kumar,[1] H. N. Alshareef,[1] and U. Schwingenschlögl[1,a)]
[1]*KAUST, Physical Science & Engineering, Thuwal 23955-6900, Kingdom of Saudi Arabia*
[2]*Department of Physics, Yildiz Technical University, 34210 Istanbul, Turkey*

(Received 13 January 2012; accepted 3 February 2012; published online 8 March 2012)

We study epitaxial $SrTiO_3$ interfaced with Nb-doped $SrTi_{1-x}Nb_xO_3$ ($x = 0$, 0.125, 0.25, 0.375, and 0.5) by full-potential density functional theory. From the electronic band structures obtained by our ab-initio calculations we determine the dependence of the induced metallicity on the Nb concentration. We obtain a monotonous increase of the carrier density with the Nb concentration. The results are confirmed by experiments for $SrTi_{0.88}Nb_{0.12}O_3$ and $SrTi_{0.8}Nb_{0.2}O_3$, demonstrating the predictive power and limitations of our theoretical approach. We also show that the Seebeck coefficient decreases monotonously with increasing temperature. © *2012 American Institute of Physics*. [http://dx.doi.org/10.1063/1.3692057]

I. INTRODUCTION

Perovskite oxides with the general formula ABO_3, where A and B denote large and small cations, respectively, have been investigated extensively since they exhibit rich physical and chemical phenomena, e.g., piezoelectricity, ferroelectricity, and ferromagnetism. This makes them attractive materials for field effect transistors, non-volatile memories, piezoelectric transducers, and optical waveguides.[1–3] Strontium titanate ($SrTiO_3$; STO) is one of the most widely used cubic perovskite oxides, owing to its chemically and compositionally stable structure and small lattice mismatch with other perovskite oxides.[4–6] It finds a wide range of applications in non-volatile resistive switching memories,[7,8] field effect transistors,[9] and memory storage devices.[10] The electronic structure of STO as obtained by reflectivity measurements reveals a band insulator with a bandgap of 3.2 eV at room temperature.[11]

Even under slight *n* or *p*-doping the electronic properties of STO are modified drastically.[12–15] For example, STO shows superconductivity at low temperature ($T_c < 0.3$ K) when Ti is partially substituted by Nb.[16] It has already been demonstrated that during synthesis of Nb-doped STO, Nb^{5+} ions occupy the Ti sites and contribute to the metallicity in the otherwise insulating material.[17] When a Nb-doped STO film is grown on pure STO, the interface states are influenced by the *n*-type Nb^{5+} donors. Only very few theoretical studies have been reported for Nb-doped STO, all of them dealing with bulk systems. In Ref. 18, the structure relaxation due to the Nb dopant and formation energies have been discussed, while Refs. 19 and 20 deal with the effective mass and conductivity. In addition, the transport properties have been investigated in Ref. 21. A profound understanding of how the charge carrier density changes with the Nb positions and concentration is crucial for controlling the overall electrical conductivity of Nb-doped STO films and utilizing them for technological applications, for example, in thermoelectrics. In this paper, we address the above issues by both density functional theory based calculations and experiments. While the experimental findings focus on the variation of the electrical conductivity and Seebeck coefficient with the temperature in Nb-doped STO films with two fixed Nb concentrations, we extrapolate this knowledge for varying Nb concentrations by our simulations. Our results demonstrate that Nb doping yields an increase of the carrier concentration and decrease of the thermoelectric response in STO based oxides.

II. METHODOLOGY

A. Experimental

Thin films of Nb-doped STO were deposited on a $LaAlO_3$ substrate, held at a temperature of 700 °C, by pulsed laser deposition of $SrTi_{0.85}Nb_{0.15}O_3$ and $SrTi_{0.80}Nb_{0.20}O_3$ targets. A KrF excimer laser (248 nm) at a power density of 75 W cm^{-2} was used for ablation in the presence of Ar gas (20 mTorr). The electrical resistivity of the film was measured in the temperature range from 5 to 350 K using a physical property measurement system (PPMS, Quantum Design, USA) and in the high temperature range from 300 to 900 K using a linear four probe technique (RZ2001i, Ozawa Sciences, Japan). The high temperature (300 to 900 K) Seebeck coefficient was also measured by the RZ2001i, using the steady state method. A temperature difference of less than 4 K was maintained in the Seebeck coefficient measurements. The room temperature carrier concentration was measured using a PPMS by sweeping the applied magnetic field (50 kOe) under a steady current of 20 A in a rectangular Hall geometry. The composition of the films was measured by high-resolution Rutherford backscattering Spectrometry (HRBS-500, Kobelco, Japan). In order to reduce the influence of O vacancies, the films were further annealed in an Ar/air mixture in a furnace by slowly increasing the temperature up to 700 °C (ramp rate of 5 °C per minute) and then cooling back to room temperature in 14 hrs.

B. Computational

We use the full-potential linearized augmented plane wave plus local orbitals method as implemented in the

a)Electronic mail: Udo.Schwingenschlogl@kaust.edu.sa.

 © 2012 American Institute of Physics

[This article is copyrighted as indicated in the article. Reuse of AIP content is subject to the terms at: http://scitation.aip.org/termsconditions. Downloaded to] IP: 109.171.137.210 On: Mon, 11 May 2015 07:14:12

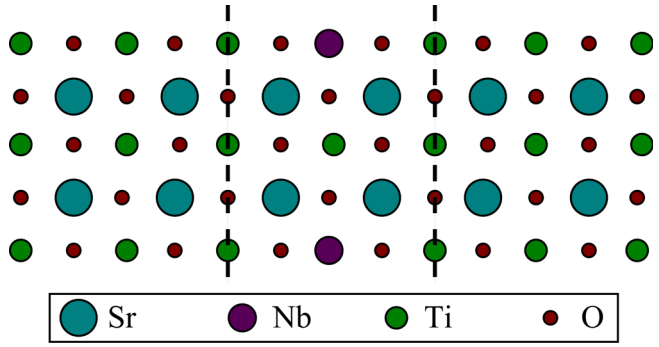


FIG. 1. (Color online) Schematic representation of the STO/$SrTi_{1-x}Nb_xO_3$/STO heterostructure ($x = 0.125$).

WIEN2k code,[22] within the framework of density functional theory. To vary the dopant concentration from $x = 12.5\%$ to 50% in $SrTi_{1-x}Nb_xO_3$, the supercell approach is used[23–26] with a $2 \times 2 \times 6$ supercell (120 atoms in total) of the primitive cubic unit cell, where 4 STO layers are considered to be the substrate (see the structure in Fig. 1). The Brillouin zone is sampled on a Monkhorst-Pack $6 \times 6 \times 2$ k-space grid. We take into account the relativistic effects for the core states, but use the scalar relativistic approximation for the valence states so that spin-orbit coupling is not included. The exchange-correlation potential is treated in the local density (LDA) and the generalized gradient (GGA) approximations. For the wave function expansion inside the atomic spheres, we choose a maximum value of $l_{max} = 12$ and employ a plane-wave cutoff of $R_{mt}K_{max} = 6$ with $G_{max} = 24$. The valence orbitals comprise Sr 4s, 5s, and 4p states, Ti 4s, 3p,

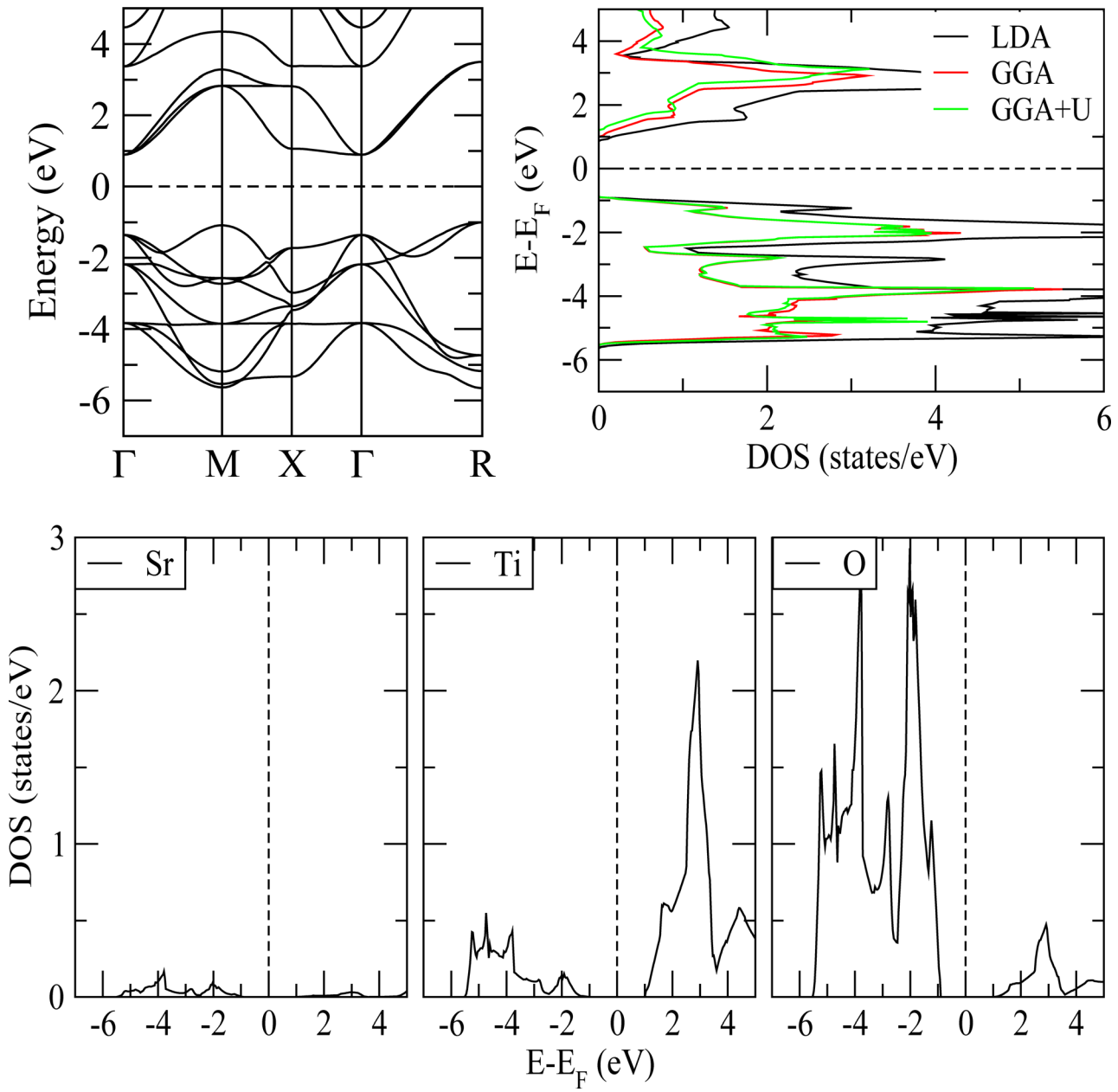


FIG. 2. (Color online) Top: Band structure and total DOS of bulk STO. Bottom: Partial Sr, Ti, and O DOSs.

[This article is copyrighted as indicated in the article. Reuse of AIP content is subject to the terms at: http://scitation.aip.org/termsconditions. Downloaded to] IP: 109.171.137.210 On: Mon, 11 May 2015 07:14:12

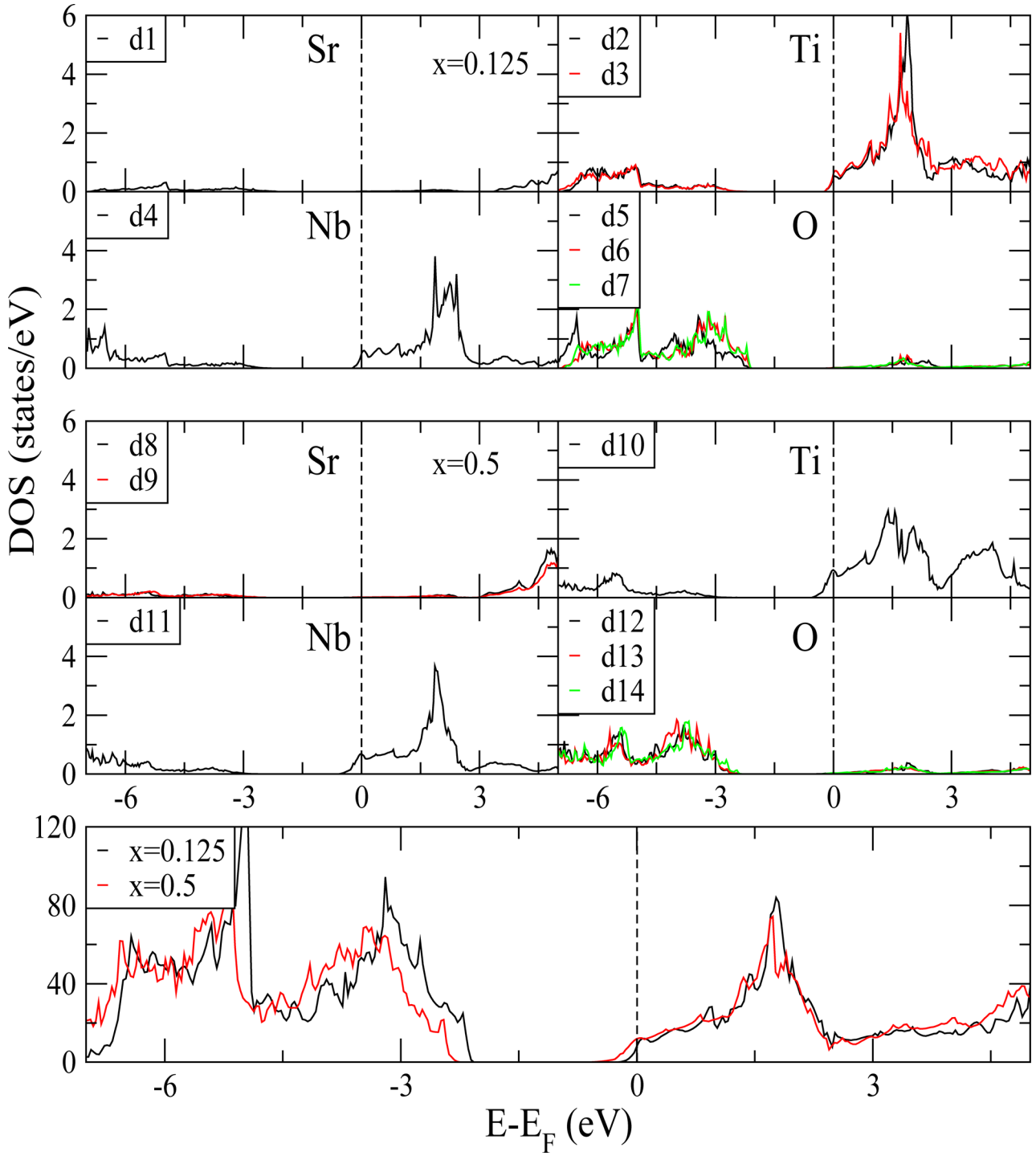


FIG. 3. (Color online) Partial Sr, Ti, Nb, and O DOSs in Nb-doped STO for doping concentrations of $x = 12.5\%$ and 50%. Atoms with varying distances from the Nb dopant are considered: $d1 = 3.44$ Å, $d2 = 5.52$ Å, $d3 = 3.90$ Å, $d4 = 0$ Å, $d5 = 1.96$ Å, $d6 = 4.36$ Å, $d7 = 5.86$ Å, $d8 = 3.39$ Å, $d9 = 3.45$ Å, $d10 = 3.99$ Å, $d11 = 0$ Å, $d12 = 1.97$ Å, $d13 = 1.99$ Å, and $d14 = 1.97$ Å. The total DOSs of the STO/$SrTi_{1-x}Nb_xO_3$/STO supercells are compared in the bottom panel.

and 3*d* states, Nb 5*s*, 4*p*, and 4*d* states, and O 2*s* and 2*p* states. All lower states are treated as semi-core and core states. The values of the muffin-tin sphere radii (in atomic units) are taken to be 2.50 for Sr, 1.94 for Ti and Nb, and 1.60 for O. All calculation parameters have been checked carefully for convergence to obtain correct results. To capture the effects of structural relaxation on the local chemical bonding and physical properties, the atomic forces in the supercell have been converged down to less than 1 mRy. In order to avoid strong Nb-Nb repulsion, we choose distances between the Nb atoms of more than 5.5 Å for all doping concentrations. Moreover, we apply the experimental lattice constant of $SrTiO_3$ ($a = 3.905$ Å). To predict the Seebeck coefficient we employ the BoltzTraP code[27] which is interfaced with WIEN2k. This code is based on Boltzmann theory and provides estimates of band structure dependent quantities (such as the electrical and thermal conductivity) within the rigid band approach.

[This article is copyrighted as indicated in the article. Reuse of AIP content is subject to the terms at: http://scitation.aip.org/termsconditions. Downloaded to] IP: 109.171.137.210 On: Mon, 11 May 2015 07:14:12

III. RESULTS AND DISCUSSION

Bulk STO is found to be insulating, compare the band structure in the top left panel of Fig. 2. The GGA bandgap is 1.9 eV, which is a well known underestimation with respect to the experimental value of 3.2 eV (Ref. 11) and in a good agreement with previous numerical findings.[28] The results for the total density of states (DOS) of bulk STO from our LDA, GGA, and GGA + U (with $U = 6$ eV) calculations are shown in the top right panel of Fig. 2. They suggest that (i) the LDA gap is smaller than the GGA gap by about 0.15 eV and (ii) the bandgap can hardly be improved by inclusion of the on-site interaction U. Hence, for all further calculations we use the GGA. Partial Sr, Ti, and O DOSs for pristine STO (bottom panels of Fig. 2) show that while the highest occupied molecular orbital is due to the O 2p states, the lowest unoccupied molecular orbital originates from the Ti 3d states. Sr hardly contributes in the energy range around the Fermi level.

We have calculated the DOS of the STO/$SrTi_{1-x}Nb_xO_3$/STO heterostructures for $x = 0.125$, 0.25, 0.375, and 0.5 to demonstrate the effect of Nb doping on the electronic structure of the system. The total and partial DOSs are shown in Fig. 3. The partial Ti and O DOSs of bulk STO (Fig. 2, bottom panel) are drastically modified in the presence of a Nb dopant. While the main contribution to the top of the valence band is due to the O 2p states with some admixtures from the Ti 3d and Nb 4d states, the main contribution to the bottom of the conduction band originates from the Ti 3d and Nb 4d states with admixtures from the O 2p states. Thus, the Nb ions contribute more to the conduction band than to the valence band. When we increase the Nb concentration, the gross shape of the DOS remains similar, but it shifts to lower energy (see Fig. 3, bottom panel). Due to hybridization with the Nb dopant, the 2p states of neighboring O atoms contribute slightly at the Fermi energy. In addition, for $x = 0.125$ the O 2p DOS is altered, especially in the valence band, depending on the O-Nb distance (see the three O atoms with distances d5, d6, and d7, for example). These O atoms hybridize a weakly with Ti and Nb, which experience strong hybridization with each other. Irrespective of the Nb-Sr distance, the Sr DOS remains mostly unchanged.

A metallic nature of the Nb-doped STO films is reflected by our experimental results for the electrical resistivity given in Fig. 4(a). The films behave as band semiconductors at low temperature. A semiconductor-to-metal transition is observed at ~200 K and ~50 K for the 12% and 20% Nb-doped film, respectively. The transition to the semiconducting state at low temperature is due to the carrier freeze-out phenomenon, i.e., not sufficient carriers are activated to the conduction band to make the system metallic. A similar transition recently has been reported at 78 K for O-deficient STO thin films.[29] The carrier concentrations of the 12% and 20% Nb-doped films are estimated to be $3.9 \cdot 10^{20}$ cm^{-3} and $8.0 \cdot 10^{20}$ cm^{-3}, respectively, at 300 K. Insight into the temperature dependence of the carrier concentration as well as mobility at high temperature would require Hall effect measurements. Generally speaking, the intrinsic charge carrier concentration at 0 K is $n = \int_{E_c}^{E_F} \mathrm{DOS}(E)dE$, where E_c is the lower edge of the conduction band. As depicted in Fig. 4(b), an almost linear increase of n as a function of the Nb concentration is found both experimentally and theoretically. However, the theoretical description systematically overestimates n and has to be corrected accordingly. Because the electrical conductivity is proportional to the carrier concentration (and therefore the Nb doping) it has a direct effect on the Seebeck coefficient, which we aim to understand in the following.

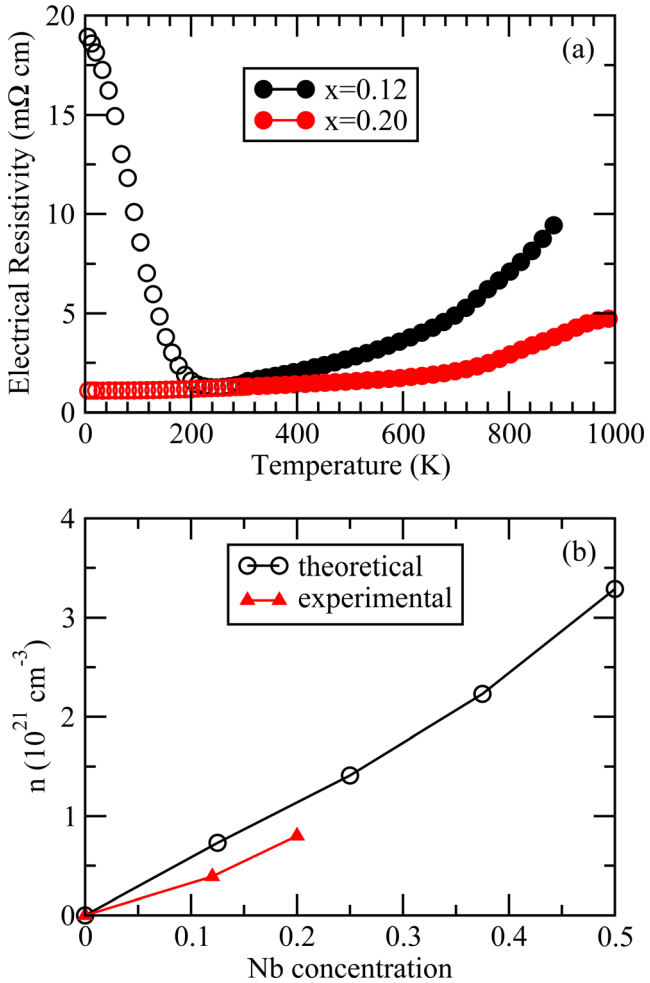


FIG. 4. (Color online) (a) Experimental temperature dependence of the electrical resistivity of Nb-doped STO films. The low temperature data is shown as open circles, the high temperature data as filled circles. (b) Carrier density as a function of the Nb concentration, comparing experiment and theory.

Within Boltzmann transport theory and the rigid band approach, as implemented in the BoltzTrap code, the thermoelectric transport tensors are given by

$$\sigma_{\alpha\beta}(T;\mu) = \frac{1}{\Omega}\int \sigma_{\alpha\beta}(\epsilon)\left[-\frac{\partial f_\mu(T;\epsilon)}{\partial \epsilon}\right]d\epsilon, \quad (1)$$

$$\nu_{\alpha\beta}(T;\mu) = \frac{1}{eT\Omega}\int \sigma_{\alpha\beta}(\epsilon)(\epsilon-\mu)\left[-\frac{\partial f_\mu(T;\epsilon)}{\partial \epsilon}\right]d\epsilon, \quad (2)$$

$$\kappa^0_{\alpha\beta}(T;\mu) = \frac{1}{e^2T\Omega}\int \sigma_{\alpha\beta}(\epsilon)(\epsilon-\mu)^2\left[-\frac{\partial f_\mu(T;\epsilon)}{\partial \epsilon}\right]d\epsilon, \quad (3)$$

[This article is copyrighted as indicated in the article. Reuse of AIP content is subject to the terms at: http://scitation.aip.org/termsconditions. Downloaded to] IP: 109.171.137.210 On: Mon, 11 May 2015 07:14:12

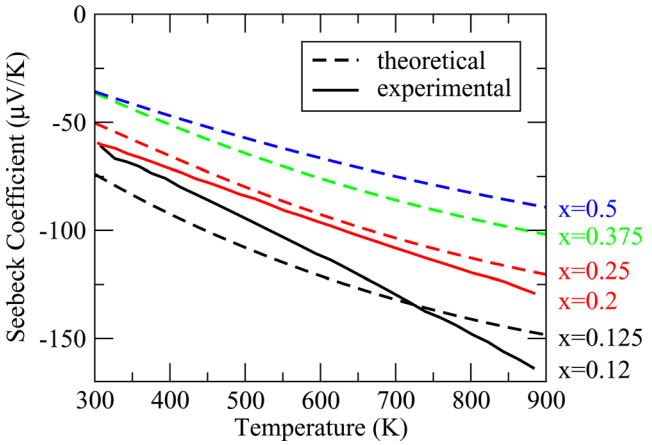


FIG. 5. (Color online) Seebeck coefficient as a function of the temperature, comparing experiment and theory.

where σ is the electrical conductivity, κ^0 is the electronic part of the thermal conductivity, f is the Fermi-Dirac distribution function, μ is the chemical potential, and T is the temperature (α, $\beta = 1, 2, 3$). The Seebeck coefficient S_{ij} is given by the electric field E_i and temperature gradient as

$$S_{ij} = E_i(\nabla_j T)^{-1} = (\sigma^{-1})_{\alpha i} v_{\alpha j}. \quad (4)$$

Taking into account the symmetry of the system ($S_{ij} = S_{ji}$), the principal Seebeck coefficient can be expressed as $S = \sigma^{-1}\nu$, where σ and ν are estimated using the rigid band approach. We present the calculated Seebeck coefficient as a function of the temperature in Fig. 5. A *n*-type state is evident from the sign of S. The Seebeck coefficient also shows a typical degenerate semiconducting nature[30] and decreases with the temperature almost linearly, resembling the behavior of bulk Nb-doped STO.[21] The absolute value of S is lower for the 20% Nb-doped film (which has the higher carrier concentration) than for the 12% Nb-doped film, at all temperatures. Similar absolute values and curvatures of the calculated and experimental S, compare Fig. 5, indicate that the Seebeck coefficient can be predicted by first principles calculations with high reliability in the full doping range.

In conclusion, we have studied the electronic band structure and thermoelectric behavior of $SrTi_{1-x}Nb_xO_3$ thin films as a function of the Nb concentration x. We have employed first- principles calculations and have compared the results to experiments for Nb concentrations of $x = 12\%$ and 20%. While undoped STO is insulating, Nb doping induces metallicity. We have determined the electron concentrations quantitatively for different Nb concentrations, both experimentally and theoretically. Our findings demonstrate the predictive power of the theoretical method as well as its limitations. We observe a prominent monotonic increase of the carrier concentration under Nb doping, which makes it possible to tailor the properties of the films. A finite but small carrier concentration is crucial for obtaining a high Seebeck coefficient.

[1]I. N. Yakovkin and M. Gutowski, Phys. Rev. B **70**, 165319 (2004).
[2]R. A. Evarestov, V. P. Smirnov, and D. E. Usvyat, Solid State Commun. **127**, 423 (2003).
[3]J. F. Scott, *Ferroelectric Memories* (Dekker, New York, 2000).
[4]J. Javier and G. Philippe, Nature **422**, 506 (2003).
[5]B. H. Lu, S. Y. Dai, Z. H. Chen, L. Yan, Y. L. Zhou, and G. Z. Yang, Chin. Sci. Bull. **48**, 1328 (2003).
[6]M. Kubo, Y Oumi, R. Miura, A. Stirling, and A. Miyamoto, Phys. Rev. B **56**, 13535 (1997).
[7]K. Szot, W. Speier, G. Bihmayer, and R. Waser, Nat. Mater. **5**, 312 (2006).
[8]T. Menke, R. Dittmann, P. Meuffels, K. Szot, and R. Waser, J. Appl. Phys. **106**, 114507 (2009).
[9]T. Sato, K. Shibuya, T. Ohniski, K. Nishio, and M. Lippmaa, J. Appl. Phys. **46**, L515 (2007).
[10]M. Copel, P. R. Duncomber, D. A. Neumayer, T. M. Shaw, and R. M. Tromp, Appl. Phys. Lett. **70**, 3227 (1997).
[11]M. Cardona, Phys. Rev. **140**, A651 (1965).
[12]X. G. Chen, X. B. Ma, Y. B. Yang, L. P. Chen, G. C. Xiong, G. J. Lian, Y. C. Yang, and J. B. Yang, Appl. Phys. Lett. **98**, 122102 (2011).
[13]S. Dai, H. Lu, F. Chen, Z. Chen, Z. Y. Ren, and D. H. L. Ng, Appl. Phys. Lett. **80**, 3545 (2002).
[14]A. Leitner, C. T. Rogers, J. C. Price, D. A. Rudman, and D. R. Herman, Appl. Phys. Lett. **72**, 3065 (1998).
[15]D. Olaya, F. Pen, C. T. Rogers, and J. C. Price, Appl. Phys. Lett. **84**, 4020 (2004).
[16]J. F. Schooley, W. R. Hosler, E. Amber, J. H. Becker, M. L. Cohen, and C. S. Koonce, Phys. Rev. Lett. **14**, 305 (1965).
[17]T. Tomio, H. Miki, H. Tabata, T. Kawai, and S. Kawai, J. Appl. Phys. **76**, 5886 (1994).
[18]R. Astala and P. D. Bristowe, J. Phys.: Condens. Matter **14**, L149 (2002).
[19]J. Yun, Z. Zhang, F. Zhang, and W. Zhao, *Proceedings of the 3rd IEEE Int. Conf. on Nano/Micro Engineered and Molecular Systems* (2008).
[20]W. Wunderlich, H. Ohta, and K. Koumoto, Physica B **404**, 2202 (2009).
[21]A. Kinaci, C. Sevik, and T. Çağin, Phys. Rev. B **82**, 155114 (2010).
[22]P. Blaha, K. Schwarz, G. Madsen, D. Kvasicka, and J. Luitz, *WIEN2k, An Augmented Plane Wave + Local Orbitals Program for Calculating Crystal Properties* (Technical University of Vienna, Vienna, 2001).
[23]S. Nazir and U. Schwingenschlögl, Appl. Phys. Lett. **99**, 073102 (2011).
[24]M. Upadhyay Kahaly, S. Nazir, and U. Schwingenschlögl, Appl. Phys. Lett. **99**, 123501 (2011).
[25]U. Schwingenschlögl and C. Schuster, EPL **86**, 27005 (2009); Chem. Phys. Lett. **467**, 354 (2009).
[26]U. Schwingenschlögl and C. Schuster, Phys. Rev. Lett. **102**, 227002 (2009).
[27]G. K. H. Madsen and D. J. Singh, Computer Physics Commun. **175**, 67 (2006).
[28]X. G. Guo, X. S. Chen, and W. Lu, Solid State Commun. **126**, 441 (2003).
[29]Z. Q. Liu, D. P. Leusink, X. Wang, W. M. Lü, K. Gopinadhan, A. Annadi, Y. L. Zhao, X. H. Huang, S. W. Zeng, Z. Huang, A. Srivastava, S. Dhar, T. Venkatesan, and Ariando, Phys. Rev. Lett. **107**, 146802 (2011).
[30]Y. I. Ravich, B. A. Efimova, and I. A. Smirov, *Semiconducting Lead Chalcogenides* (Plenum, New York, 1970).

[This article is copyrighted as indicated in the article. Reuse of AIP content is subject to the terms at: http://scitation.aip.org/termsconditions. Downloaded to] IP: 109.171.137.210 On: Mon, 11 May 2015 07:14:12